Available online at www.sciencedirect.com

SciVerse ScienceDirect

Procedia IUTAM 00 (2012) 000-000

Procedia IUTAM

www.elsevier.com/locate/procedia

Topological Fluid Dynamics II

Quantifying entanglement for collections of chains in periodic boundary conditions models

E. Panagiotou[a], K.C. Millett[b], S. Lambropoulou[a]

[a]*Department of Mathematics, National Technical University of Athens, Zografou Campus, Athens GR 15780, Greece*
[b]*Department of Mathematics, University of California, Santa Barbara, CA 93106, USA*

Abstract

Using the Gauss linking integral we define a new measure of entanglement for a collection of closed or open chains, the *linking matrix*. For a system employing periodic boundary conditions (PBC) we use the periodic linking number and the periodic self-linking number to define the *periodic linking matrix*. We discuss its properties with respect to the cell size used for the simulation of a periodic system and we propose a method to extract from it information concerning the homogeneity of the entanglement. Our numerical results on systems of equilateral random walks in PBC indicate that there is a cell size beyond which the dependence of some properties of the periodic linking matrix on cell size vanishes and that the eigenvalues of the linking matrix can measure the homogeneity of the entanglement of the constituent chains.

Keywords: linking matrix; periodic linking matrix; periodic boundary conditions; homogeneity; polymers; helicity; asphericity; Cheeger constant

1. Introduction

Polymer melts are *complex fluids*, exhibiting both liquid and solid like behaviour. The uncrossability of the polymer chains that compose a melt gives rise to *entanglement* which is closely related to the viscoelastic properties of materials [1, 2]. Under certain conditions, polymer chains can be seen as closed or open mathematical curves in space whose topological and geometrical complexity can be measured [3, 4, 5, 6, 7]. Similarly, vortex lines in a fluid flow may be seen as mathematical curves that are linked or knotted [8, 9, 10], properties that help characterize the system. Polymer and vortex entanglement share some common features, especially when there is mutual interference, as in the case of polymer solutions. The addition of small amounts of long chain polymers to flowing fluids produces large effects on a wide range of phenomena such as the stability of laminar motion, transition to turbulence, vortex formation and break-up, turbulent transport of heat, mass and momentum, and surface pressure fluctuations [11].

A classical measure of entanglement is the Gauss linking integral, a topological invariant in the case of closed chains. The linking number is closely related to the *helicity* of the fluid flow, which is an invariant property of invis-

* Corresponding author. Tel.: +0-000-000-0000 ; fax: +0-000-000-0000 .
E-mail address: panagiotou@math.ntua.gr

cous liquids [8]. For open or mixed chains, the Gauss linking integral is a real number that is characteristic of a fixed configuration and changes continuously under continuous deformations of the constituent chains [7]. In order to measure the global entanglement in systems composed by many chains, more complex invariants are needed. However, the local entanglement characteristics of the systems may provide important information concerning viscoelasticity or turbulence [6, 12]. In this paper we define the *linking matrix*, as a measure of the entanglement of a collection of closed or open chains, and we use its eigenvalues to provide information about the homogeneity of the entanglement.

When modelling a physical system periodic boundary conditions (PBC) are applied in order to eliminate boundary effects, as for example in the study of polymer melts, or in studies of turbulence. In a PBC model, the cubical simulation box is replicated throughout space to form an infinite lattice. In the course of the simulation, when a molecule moves in the central box, its periodic image in every one of the other boxes moves in exactly the same way. Thus, as a molecule leaves the central box, one of its images will enter through the opposite face. In the case of a periodic system a different measure of entanglement is needed in order to capture all the topological constraints and the effect of the periodicity of the conformations [13, 14, 15]. In [16, 17] we defined the *periodic linking number* for curves in PBC [17]. In this paper we use the periodic linking number and the periodic self-linking number to define a *periodic linking matrix*. We study its eigenvalues and its dependence on the simulation cell size, which may be related to finite size effects in simulations [17].

In Section 2 we give some basic definitions for systems employing PBC. In Section 3 we recall the definitions of linking number and periodic linking number and we examine their relation to helicity. In Section 4 we define the linking matrix and the periodic linking matrix and discuss their properties. In Section 5 we provide some numerical results on equilateral random walks for various systems.

2. Systems employing PBC

In [16] we defined a *cell* to be a cube with n arcs embedded into it such that arcs may terminate only in the interior of the cube or on a face, but not on an edge or corner, and those arcs which meet a face satisfy the PBC requirement that opposite faces of the cell have exactly the same intersection structure. A cell generates a *periodic system* in 3-space by tiling 3-space with the cubes so that they fill space and only intersect on their faces. This allows an arc in one cube to be continued across a face into an adjacent cube and so on. Without loss of generality, we choose a cell of the periodic system that we call *generating cell*. Then any other cell in the periodic system is a translation of the generating cell by a vector $\vec{c} = (c_x, c_y, c_z), c_x, c_y, c_z \in L_{Cb}\mathbb{Z}$, where L_{Cb} is the length of an edge of the cell. A *generating chain* is the union of all the segments inside the cell the translations of which define a maximal connected arc in the periodic system. For each arc of a generating chain we choose an orientation such that the translations of all the arcs would define an oriented arc in the periodic system.

For generating chains we shall use the symbols $i, j, \ldots$. An *unfolding* of a generating chain is a connected arc in the periodic system composed by exactly one translation of each arc of the generating chain. A generating chain is said to be closed (resp. open) when its unfolding is a closed (resp. open) chain. The smallest union of the copies of the cell needed for one complete unfolding of a generating chain shall be called the *minimal unfolding*. The collection of all translations of the same generating chain i shall be called a *free chain*, denoted I. A free chain is identified with the collection of its connected components. For free chains we will use the symbols $I, J, \ldots$. An *image* of a free chain is any arc in that collection that is the unfolding of one generating chain. For images of a free chain, say I, we will use the symbols $I_1, I_2, \ldots$. For example in Fig.(1(a)) and Fig.(1(b)), I_1 is an image of the free chain I. A free chain whose images in the periodic system get connected to form infinite arcs shall be called an *infinite free chain*. In case of an infinite free chain, we will call $\mathscr{I}_1, \mathscr{I}_2, \ldots$ each infinite connected component formed by a collection of images of I. For example in Fig.(1(b)) the infinite curve on which the image I_1 lies is called $\mathscr{I}_1$.

Given a cell C we can create larger cells that generate the same system. For example, if C is a cell with one PBC, then if we concatenate along a face of C which imposes PBC another copy of it, we form a larger cell that we denote $2C$. Then we can glue copies of $2C$ in order to create the same periodic system. In the general case of a system that imposes three PBC, we can form a new cell by concatenating the surrounding 26 translations of C, we denote again as $2C$. The cell mC in this case is the cell formed by $(2m+1)^3$ copies of C. In [17] is proved that if the cell C has n generating chains, then the cell C' that results by gluing m copies of C respecting the PBC, has mn generating chains.

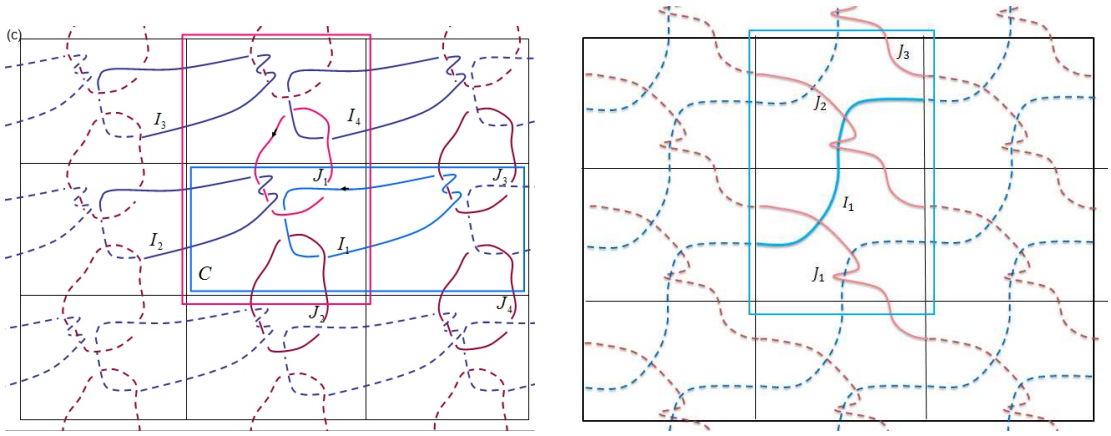

Fig. 1. The central cell C and the periodic system it generates. (a) The case of closed or open free chains. The generating chain i (resp. j) is composed by the blue (resp. red) arcs in C. The free chain I (resp. J) is the set of blue (resp. red) chains in the periodic system. Highlighted are the minimal unfoldings of the images I_1 and J_1. (b) The case of infinite free chains. The free chain I (resp. J) is composed by all the blue (resp. red) arcs in the periodic system. Now each connected component defines an infinite curve, say $\mathscr{I}$ ($\mathscr{J}$ resp.). The highlighted arc in blue is the image I_1 of I.

3. The periodic linking number

The Gauss *linking number* of two disjoint oriented curves l_1 and l_2, whose arc-length parametrization is $\gamma_1(t), \gamma_2(s)$ respectively, is defined as a double integral over l_1 and l_2:

$$lk(l_1,l_2) = \frac{1}{4\pi}\int_{[0,1]}\int_{[0,1]} \frac{(\dot\gamma_1(t),\dot\gamma_2(s),\gamma_1(t)-\gamma_2(s))}{|\gamma_1(t)-\gamma_2(s)|^3}dtds \tag{1}$$

where $(\dot\gamma_1(t),\dot\gamma_2(s),\gamma_1(t)-\gamma_2(s))$ is the triple product of $\dot\gamma_1(t),\dot\gamma_2(s)$ and $\gamma_1(t)-\gamma_2(s)$.

In the case of closed chains the Gauss linking number is a topological invariant. If it is equal to zero, the two chains are said to be algebraically unlinked. For open chains the Gauss linking number is a continuous function in the space of configurations and as the endpoints of the chains tend to coincide, it tends to the linking number of the resulting closed chains. For open chains, lk may not be zero, even for chains whose convex hulls do not intersect. But as the distance between them increases, lk tends to zero.

The Gauss linking number is related to the helicity of a fluid as follows [8]: Let $\vec u(\vec x,t)$ be the velocity field in an inviscid incompressible fluid, and let $\vec\omega(\vec x,t) = \nabla\times\vec u$ be the corresponding vorticity field, which is zero except in two closed vortex filaments of strengths κ_1,κ_2, whose axes are C_1,C_2. Let S be any closed orientable surface moving with the fluid on which $\vec u\cdot\vec n = 0$. Then the *helicity* is

$$H = \int_V \vec u\cdot\vec\omega\, dV = 2lk(C_1,C_2)\kappa_1\kappa_2 \tag{2}$$

where V is the volume inside S. This is an invariant for inviscid incompressible fluids. The integral in the left hand side is over the entire volume of the fluid or over any other volume whose boundary is a surface for which $\vec u\cdot\vec v = 0$. As we discussed in the previous paragraph, the linking integral can be computed even if the arcs C_1,C_2 are not closed in V, but then this is a continuously varying measure. However the case where C_1,C_2 are not entirely contained in V is of interest. In [18] it was shown that in some cases the linking of the open arcs in V of the vortex lines C_1,C_2, is related to the difference in helicities of any two field configurations that differ only inside V, which is an invariant quantity. Thus, the volume V's contribution to the overall helicity of a field has a well-defined relative measure. When applied to smaller volumes than rather on the entire volume of the fluid, information is provided about the distribution of helicity in a fluid and its relation to turbulence [18, 19].

In [17] we apply the Gauss linking number and its extension to open chains to the situation of chains defined in a PBC model, thereby providing a measure of the large scale entanglement between two free chains:

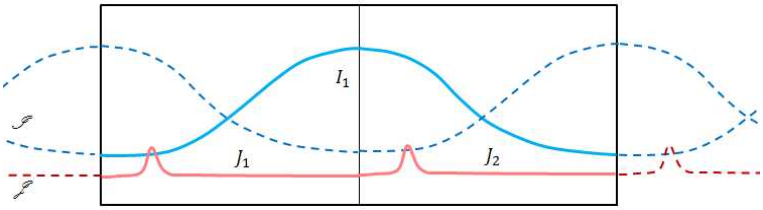

Fig. 2. The linking number between the two infinite lines $\mathscr{I}$, $\mathscr{J}$ is related to the periodic linking number as: $LK_P(I,J) = \lim_{T\to\infty} \frac{lk(\mathscr{I}_T,\mathscr{J})}{T}$, where $\mathscr{I}_T$ is the arc formed by T concatenated copies of I_1.

Definition 1 (Periodic linking number) *Let I and J denote two free chains in a periodic system. Suppose that I_1 is an image of the free chain I in the periodic system. The periodic linking number, LK_P, between two free chains I and J is defined as:*

$$LK_P(I,J) = \sum_u lk(I_1, J_u) \tag{3}$$

where the sum is taken over all the images J_u of the free chain J in the periodic system.

As it turns out [17], LK_P is symmetric. In the case of closed chains LK_P is an integer topological invariant and it is equal to the intersection number between the 2-chain and the 2-cycle formed by the arcs of the generating chains in the 3-manifold defined by identifying the opposite faces of the cell with respect to the PBC [17]. For a system of two line vortices C_1, C_2 of strengths κ_1, κ_2 in PBC, such that the corresponding two generating chains are closed, the helicity in a volume bounded by a surface on which $\vec{u}\cdot\vec{n} = 0$, inside the corresponding 3-manifold defined by the cell, would be related to the periodic linking number as follows:

$$H = \int_V \vec{u}\cdot\vec{\omega}\, dV = 2LK_P(C_1, C_2)\kappa_1\kappa_2 \tag{4}$$

In the case of open chains, LK_P is an infinite summation which converges [17]. Thus the periodic linking number extends directly to both open and infinite chains, for which it is a real number, and it is a continuous function in the space of configurations.

We notice that there is a connection between the periodic linking number of two infinite free chains and the Gauss linking number of two infinite components of these free chains. Consider the example of two infinite free chains I, J in a system with one PBC shown in Fig.(2). Let $\mathscr{I}$, $\mathscr{J}$ denote two infinite arcs formed by the images of I and J respectively. Then we have the following:

$$lk(\mathscr{I},\mathscr{J}) = \sum_{t=1}^{\infty}\sum_{u=1}^{\infty} lk(I_t, J_u) = \lim_{T\to\infty}\sum_{t=1}^{T}\sum_{u=1}^{\infty} lk(I_t, J_u) = \lim_{T\to\infty}\sum_{t=1}^{T} LK_P(I,J) \tag{5}$$

since $LK_P(I,J)$ is independent of the image of I (or J) used for its computation. Thus, in this example, the periodic linking number between I and J is related to the linking number of $\mathscr{I}$, $\mathscr{J}$ as follows:

$$LK_P(I,J) = \lim_{T\to\infty} \frac{lk(\mathscr{I}_T,\mathscr{J})}{T} \tag{6}$$

where $\mathscr{I}_T$ denotes the arc that is formed by taking T consecutive copies of I_1 in $\mathscr{I}$.

In the case of the trajectories of the phase flow of a divergence-free field, Arnol'd defined the asymptotic linking number, $\Lambda(x_1, x_2)$, of a pair of these trajectories, and showed that it converges and that the mean value of $\Lambda(x_1, x_2)$ is equal to the asymptotic Hopf invariant, the helicity [20]. The relation of the periodic linking number of infinite chains with the Gauss linking number and the asymptotic linking number will be discussed in a sequel to this paper.

In many cases the local topological constraints are more important than the global linking of the chains [6, 19]. For this reason in [16] we defined the *local periodic linking number*, $LK(I,J)$, where for an image I_1 of I we take into

consideration only the images of J that intersect its minimal unfolding. For example, in Fig.(1(a)) for the computation of the local periodic linking number, $LK(J,I)$, we have $LK(J,I) = lk(J_1,I_1) + lk(J_1,I_2) + lk(J_1,I_3) + lk(J_1,I_4)$. We can see that $lk(I_1,J_1) = lk(J_1,I_1), lk(I_1,J_2) = lk(J_1,I_4), lk(I_1,J_3) = lk(J_1,I_2)$ and $lk(I_1,J_4) = lk(J_1,I_3)$, thus $LK(I,J) = LK(J,I)$. In [16] we used the local periodic linking number to study the effect of the CReTA (Contour Reduction Topological Analysis) algorithm [6] on the entanglement of open polymer chains, a study that may be relevant to the study of helicity obstruction in energy relaxation [21, 22]. Our numerical results in [16] showed that the normalized probability distribution of LK for the original and reduced systems is the same. The definition of the local periodic linking number can be adapted to the case of infinite free chains. For example, in Fig.(1(b)) $LK(I,J) = lk(I_1,J_1) + lk(I_1,J_2) + lk(I_1,J_3)$.

In systems employing PBC, a chain may be entangled with its own periodic images. We propose the following definition of self-linking in PBC:

Definition 2 (Periodic self-linking number) *Let I denote a free chain in a periodic system and let I_1 be an image of I, then the periodic self-linking number of I is defined as:*

$$SL_P(I) = sl(I_1) + \sum_{u \neq 1} lk(I_1, I_u) \tag{7}$$

where the index u runs over all the images of I, except I_1, in the periodic system, and where sl denotes the classical self-linking number [23, 24].

The periodic self-linking number can be applied to closed, open or infinite free chains. In the case of a closed free chain, the periodic self-linking number is equal to the intersection number of the 2-chain and the 2-cycle formed by its normal push-off in the identification space [17].

For a knotted vortex filament C_1 whose strength is κ_1 the helicity in a volume bounded by a surface on which $\vec{u} \cdot \vec{n} = 0$, is: $H = sl(C_1)\kappa_1^2$ [8, 9]. For a vortex filament in PBC, such that the corresponding generating chain is closed, the helicity in a volume bounded by a surface on which $\vec{u} \cdot \vec{n} = 0$, inside the corresponding 3-manifold defined by the cell, is related to the periodic self-linking number as $H = SL_P(C_1)\kappa_1^2$.

4. The linking matrix

In [17] we used the linking number to define a measure of entanglement of the entire collection of chains that span a physical system, namely:

Definition 3 *The linking matrix , LM, of a collection of chains, say $I, J, \ldots, W$, is defined to be the matrix with elements $a_{ij} = lk(I,J)$ if $i \neq j$ and $a_{ii} = sl(I)$.*

Since the linking number is symmetric, this is a symmetric matrix. The linking matrix takes into consideration the first order linking information of the system, and can be computed both for closed and open chains. An interpretation of this matrix as an operator could be very helpful but this remains elusive, since the appropriate operation under which the space of knots and links would be a vector space is still unknown. Nevertheless, LM is a real symmetric matrix and its eigenvalues are real numbers. In the case of closed chains, they are integers invariant under continuous deformations of the chains.

A linking matrix can be also created for a system of line vortices $C_1, C_2, \ldots, C_n$. Let us multiply the $ij-$th element of the matrix, for $i \neq j$, by $\kappa_i\kappa_j$, the strengths of the line vortices C_i and C_j respectively, and multiply the $i-$th diagonal element by κ_i^2. Then the sum of all the elements of the linking matrix is equal to the helicity of the system.

For a cell C that generates a periodic system, we further defined in [17]:

Definition 4 *The periodic linking matrix, LM_C, for a cell C that generates a periodic system, is the matrix with elements $a_{ij} = LK_P(I,J)$ if $i \neq j$ and $a_{ii} = SL_P(I)$.*

For a system simulated by a cell with n generating chains, LM_C is of size $n \times n$. Thus the periodic linking number enables us to reduce the study of the entanglement of an infinite collection of chains that compose the periodic system

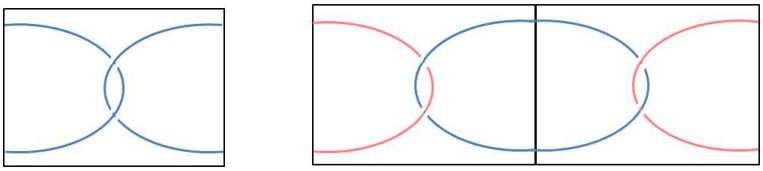

Fig. 3. (a) The cell C is composed by one generating closed chain, say i, to which it implies one PBC. There are two images of I, say I_1, I_2 that intersect C. The size of the corresponding periodic linking matrix is 1×1. (b) The cell $2C$ contains two generating chains, $i^{(1)}$ (the blue arcs) and $i^{(2)}$ (the red arcs) to which it imposes one PBC. The size of the corresponding periodic linking matrix is 2×2.

to the study of a finite dimensional matrix. In particular, for line vortices in PBC we can also compute the helicity using the periodic linking matrix.

We notice now that the linking matrix depends on the size of the cell used for the simulation of a system. Let us, for example, consider a cell C with one PBC composed by n generating chains, and let LM_C denote the corresponding periodic linking matrix of dimension $n \times n$. Next, let $C' = mC$ denote the cell that is created by gluing m copies of C respecting the PBC. It follows that the corresponding periodic linking matrix, $LM_{C'}$ is of dimension $mn \times mn$ (see Fig.(3) for an illustrative example). Indeed, the cells C and C' describe different topological objects. Namely, if we identify the opposite faces of the cell, then we will get an $n-$component link in a $3-$manifold in the first case and a $mn-$component link in the same $3-$manifold in the second case. So, we notice that the linking matrices LM_C and $LM_{C'}$ are different, but the periodic system that the cells generate and whose entanglement we wish to measure is the same. We will discuss the dependence of the periodic linking matrix on the cell size and also quantities that remain invariant of the cell size. The following is proved in [17]:

Proposition 5 *Consider n free chains in the periodic system formed by a cell C with three PBC. Then for the periodic linking matrix LM_{mC} of the cell mC made from $(2m+1)^3$ copies of C, we have*

$$LM_{mC} = \begin{bmatrix} LM_C & D \\ 0 & E \end{bmatrix} \tag{8}$$

where D is of dimension $n \times \Big((2m+1)^3 - 1\Big)n$ and E is of dimension $\Big((2m+1)^3 - 1\Big)n \times \Big((2m+1)^3 - 1\Big)n$.

Notice that, from this result, it follows that the eigenvalues of LM_C are among the eigenvalues of LM_{mC} for all m, indicating that they capture a property of the periodic system that is independent of cell size.

We propose to use the eigenvalues of the linking matrix as a measure of the homogeneity of the entanglement in a physical system . For this purpose, we employ methods and ideas from graph theory. A weighted undirected graph $G = (V, E)$ (possibly with loops) has associated with it a weight function $w : V \times V \to \mathbb{R}$ satisfying $w(u,v) = w(v,u)$ and $w(u,u) \geq 0$. We note that if $\{u,b\} \notin E$, then $w(u,v) = 0$. We represent a system of chains by a weighted graph as follows: We represent each chain by a vertex. Then two vertices are connected with an edge if their absolute linking number is greater than zero. Also, there is an edge of a vertex to itself if the chain has absolute self-linking number greater than zero. Each edge of this graph has an associated weight function that is defined as $w(u,v) = |lk(u,v)|$ and $w(u,u) = |sl(u)|$. In the case of a periodic system, each vertex represents a generating chain, and the weight function is defined as $w(u,v) = |LK_P(u,v)|$ and $w(u,u) = |SL_P(u)|$.

As we shall see, the homogeneity of the entanglement in a physical system can be related to the connectivity of the corresponding weighted graph. In the case of polymer melts, the effects of inhomogeneity in the entanglement have been reported in shear stress experiments [25]. In the study of turbulent flow the helicity integral can be applied to some part of a region of vortical flow in order to analyze the motion of limited lengths of vortex tubes where they interact with other vortices [18, 19]. The linking matrix of the corresponding vortices or polymer chains can detect inhomogeneities of the entanglement in such systems. The Cheeger constant and the eigenvalues of the Laplacian of the corresponding graph can measure the extent to which this property is present and, thus, they provide information about the homogeneity of the entanglement.

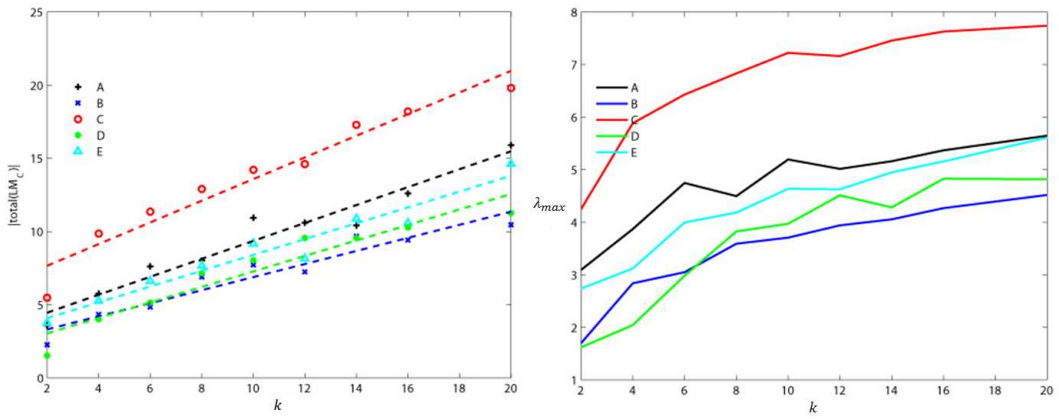

Fig. 4. Data concerning the systems: A: $N = 100$, 3 PBC, $\rho = 0.84$, B: $N = 100$, 3 PBC, $\rho = 0.5$, C: $N = 200$, 3 PBC, $\rho = 0.84$, D: $N = 100$, 1 PBC, 2 layers 0% overlap, E: $N = 100$, 1 PBC, 2 layers 50% overlap. Analysis with respect to cell size, where k denotes the number of generating chains in a cell. (a) The average absolute total sum of the elements of the matrix, $|Total(LM_C)|$. Data fitted to function of the form $a*k+b$, where $a_B < a_D < a_E < a_A < a_C$. (b) The average absolute maximum eigenvalue, λ_{max}. For $k \geq 6$, $(\lambda_{max})_B < (\lambda_{max})_D < (\lambda_{max})_E < (\lambda_{max})_A < (\lambda_{max})_C$.

5. Numerical results

In this section we analyze numerical data concerning the following systems:
(A) Equilateral random walks of length $N = 100$ in a cell with three PBC, at density $\rho = 0.84$. (where the density is defined as N/V, where N is the total number of vertices and V the volume of the cell), (B) Equilateral random walks of length $N = 100$ in a cell with three PBC, at density $\rho = 0.5$, (C) Equilateral random walks of length $N = 200$ in a cell with three PBC, at density $\rho = 0.84$, (D) Equilateral random walks of length $N = 100$ in a cell with one PBC, at density $\rho = 0.84$, separated in two layers that do not overlap, (E) Equilateral random walks of length $N = 100$ in a cell with one PBC, at density $\rho = 0.84$, separated in two layers that overlap by 50% and (F) Polyethylene (PE) melts, that consist of PE chains of length $N = 1000$ in a cell with three PBC, at density $\rho = 0.78 g/cm^3$ (PE data generated by C. Tzoumanekas).

For these systems, we compute the periodic linking matrices for the corresponding end-to-end closed chains. Our numerical results in [17] suggest that the total torsion of a chain is much larger than the absolute value of its linking number with other images. For this reason, in order to make the linking distribution in the system more evident, we will ignore the self-linking number of the chains and use only the linking with periodic self-images for the diagonal elements of the matrix.

For the systems (A)-(E), we generate samples at different cell size and study their periodic linking matrices. For each one of these systems we start with a sample of cells $C_i, i = 1, \ldots 100$, such that there are two generating chains in C_i for all i. Next, for each system we generate a new sample of cells $C'_i, i = 1, \ldots, 100$ each of which contains 4 generating chains. Similarly, the k_1-th sample consists of cells with $k = 2k_1$ generating chains. The PE data (system (F)) concerns 80 cells with $k = 8$ generating chains each.

First we study the scaling of the average absolute value of the sum of all the elements of the linking matrix over all conformations with respect to the cell size (Fig.(4(a))). We denote it $|Total(LM_C)|$. In [17] it is proved that this quantity scales linearly with cell size. Indeed, our numerical data confirm that. For each system the data is fitted to a curve of the form $a*k+b$, with (A): $a = 0.612484$, $b = 3.23239$, (B): $a = 0.446629$, $b = 2.4189$, (C): $a = 0.739565$, $b = 6.18445$, (D): $a = 0.52917$, $b = 1.98174$, (E): $a = 0.540258$, $b = 3.00181$, for each system respectively. We observe that $a_B < a_D < a_E < a_A < a_C$. This suggests that $|Total(LM_C)|$ dependents on the density, the number of chains and the length of the chains. The corresponding value for the PE frames is $|Total(LM_C)_{PE}| = 19$. This corresponds to the point with coordinates $(8, 19)$, which shows that $|Total(LM_C)_{PE}|$ is larger than the values of $|Total(LM_C)|$ of the other systems at $k = 8$. This is expected, since the PE data concern much longer chains. We note that a similar quantity has been studied in [12] for chains in 3-space and numerical studies therein showed that it grows with respect to the density and the number of chains.

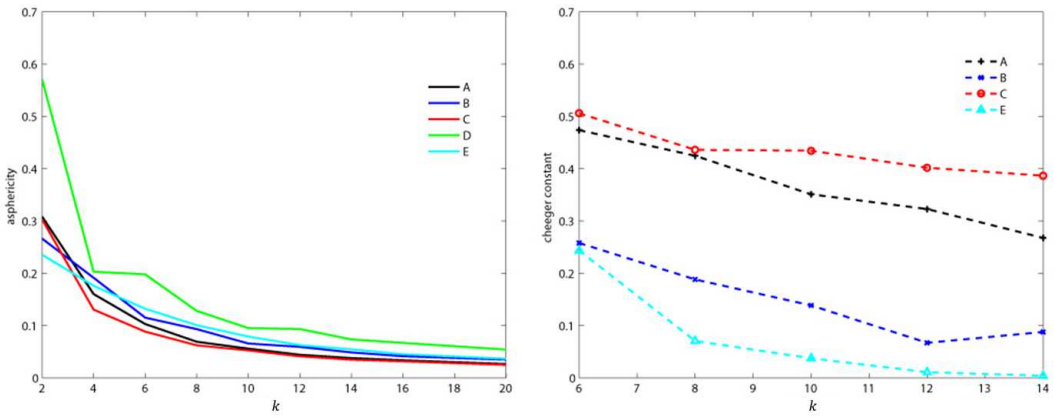

Fig. 5. Data concerning the systems: A: $N = 100$, 3 PBC, $\rho = 0.84$, B: $N = 100$, 3 PBC, $\rho = 0.5$, C: $N = 200$, 3 PBC, $\rho = 0.84$, D: $N = 100$, 1 PBC, 2 layers 0% overlap, E: $N = 100$, 1 PBC, 2 layers 50% overlap. Analysis with respect to cell size, where k denotes the number of generating chains in a cell. (a) The average asphericity of the eigenvalues of the periodic linking matrix. The average asphericity of the system D is larger than the rest. (b) The average Cheeger constant, $0 = (h_G)_D < (h_G)_E < (h_G)_B < (h_G)_A < (h_G)_C$ at all cell sizes.

Next, we compute the average value of the largest absolute eigenvalue of the periodic linking matrix over all conformations (Fig.(4(b))) at each cell size. We notice that by Proposition 5, we expect that some of the eigenvalues of the periodic linking matrix are independent of cell size, but we do not know which ones. We see that the largest eigenvalue increases in all cases and we notice a similar scaling for all systems. For $k \geq 6$ the values of the average maximum eigenvalue for each system are related as $(\lambda_{max})_B < (\lambda_{max})_D < (\lambda_{max})_E < (\lambda_{max})_A < (\lambda_{max})_C$, which coincides with the ordering of the systems with respect to $|Total(LM_C)|$. Thus the largest eigenvalue depends on the density, the number of chains and the length of the chains. The corresponding value for the PE frames is $(\lambda_{max})_{PE} = 8.0756$, which is larger than the other systems at $k = 8$. This is expected since the PE chains are longer.

The *asphericity* of the eigenvalues of a matrix of size $n \times n$ is defined as [27, 28]:

$$A_n = \frac{1}{n-1} \frac{\sum_{i>j}^{n} < (\lambda_i^2 - \lambda_j^2)^2 >}{< (\sum_i \lambda_i^2)^2 >} \tag{9}$$

where λ_i are the eigenvalues of the matrix and it can be used as a measure of the relative variance of the eigenvalues of the matrix. Fig.(5(a)) shows the scaling of the average asphericity over all configurations with respect to cell size. We notice that the asphericity of all the systems decreases with cell size and tends to an asymptotic value, which, for $k \geq 6$, is different for each system. The asphericity of system D is larger than the asphericity of all the other systems at all cell sizes. Recall that system D is composed of two non-intersecting layers of chains. This suggests that the asphericity can distinguish between the homogeneous and non-homogeneous systems. The corresponding value for the PE frames is 0.028539, which is smaller than all the other systems at the corresponding cell size, indicating a larger homogeneity for longer chains.

Next, we compute the average value of the *Cheeger constant* [26] of the periodic linking matrix over all configurations for each system at each cell size. For $k \geq 6$, the values of the different systems do not overlap. The results for the systems A, B, C, E are shown in Fig.(5(b)). The system D is not shown in the figure, since we know that $(h_G)_D = 0$ at all cell sizes, because it consists of two layers of chains that do not overlap, thus the corresponding weighted graphs have two components. Due to the computational cost of the Cheeger constant, the maximum cell size is $k = 14$. In Fig.(5(b)) we notice a similar scaling for all systems, decreasing with cell size. Also, we notice that $0 = (h_G)_D < (h_G)_E < (h_G)_B < (h_G)_A < (h_G)_C$ at all cell sizes. System E concerns two layers of chains that overlap only by 50% and its value is smaller than the rest, which shows that the Cheeger constant can detect the inhomogeneity in the structure. We observe also a difference for the other systems which have no restriction on homogeneity by construction, but differ on the length of the chains. This demonstrates that the entanglement in systems with longer chains is more homogeneous.

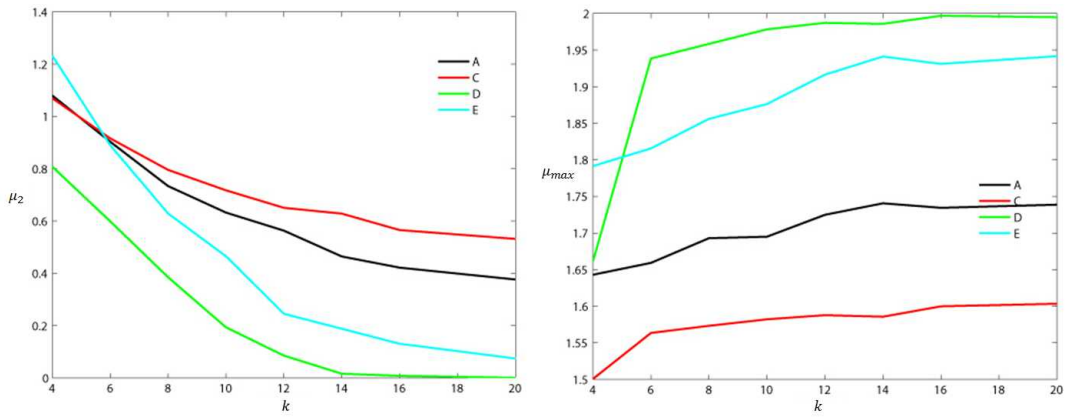

Fig. 6. Data concerning the systems: A: $N = 100$, 3 PBC, $\rho = 0.84$, C: $N = 200$, 3 PBC, $\rho = 0.84$, D: $N = 100$, 1 PBC, 2 layers 0% overlap, E: $N = 100$, 1 PBC, 2 layers 50% overlap. Analysis with respect to cell size, where k denotes the number of generating chains in a cell. (a) The average second smallest eigenvalue, $(\mu_{min})_2$, of the Laplacian of the graph that corresponds to the periodic linking matrix. For $k \geq 6$, $(\mu_2)_D < (\mu_2)_E < (\mu_2)_A < (\mu_2)_C$. (b) The average largest eigenvalue, μ_{max}, of the Laplacian of the graph of the periodic linking matrix. For $k \geq 6$, $(\mu_{max})_C < (\mu_{max})_A < (\mu_{max})_E < (\mu_{max})_D$.

As the computation of the Cheeger constant is computationally difficult, one may prefer to use the Laplacian of the weighted graph corresponding to the periodic linking matrix, to obtain information about the homogeneity of the entanglement. For example, the second smallest eigenvalue of the Laplacian of the graph, μ_2, is related to the Cheeger constant by the Cheeger inequality: $2h_G \geq \mu_2 \geq \frac{h_G^2}{2}$ [26]. Fig.(6(a)) shows the average value of the second smallest eigenvalue of the Laplacian matrix of the graph that corresponds to the periodic linking matrix over all configurations for the systems A, C, D, E. We observe that the average value of μ_2 decreases for all systems with respect to cell size, approaching an asymptotic value. For $k \geq 6$ the values of the different systems are different at all cell sizes, with $(\mu_2)_D < (\mu_2)_E < (\mu_2)_A < (\mu_2)_C$. This ordering is similar to that obtained for the Cheeger constant in the previous paragraph. For $k \geq 14$, $(\mu_2)_D \approx 0$, as expected, since $(h_G)_D = 0$. For the PE data, $(\mu_2)_{PE} = 0.98628$, which is larger than the rest of the data at $k = 8$. Thus the Cheeger constant and the second smallest eigenvalue of the system can measure the homogeneity of a system, and our data suggest that the entanglement in systems with longer chains is more homogeneous.

The largest eigenvalue of the Laplacian of the graph that corresponds to the periodic linking matrix can also provide information about the homogeneity of the entanglement. Namely, for a graph of n vertices without isolated vertices $\mu_{max} \geq \frac{n}{n-1}$ and if $\mu_{max} = 2$ then G is bipartite [26]. Fig.(6(b)) shows the average largest eigenvalue of the Laplacian matrix over all conformations, with respect to the size of the cell. We observe that for all systems the average value of μ_{max} is greater than 1.5, which means that there are no isolated vertices in the graphs, that is, on average, there are no chains that have no linking with any other chain in the melt. Indeed, this is not something that we expect to happen for these systems. The value of μ_{max} increases for all systems until it reaches an asymptotic value. For all $k \geq 6$, the values of μ_{max} are different at each cell size and $(\mu_{max})_C < (\mu_{max})_A < (\mu_{max})_E < (\mu_{max})_D$. For $k \geq 14$, $(\mu_{max})_D \approx 0$ which indicates that system D exists a connected component that is bipartite. Indeed, this system corresponds to two layers of chains which do not overlap. As the cell size increases, chains appear that are too distant to have non-zero linking, giving rise to a bipartite graph. Thus μ_{max} can measure the homogeneity of the systems, indicating that the entanglement in systems that are composed by longer chains is more homogeneous. For the PE frames $(\mu_{max})_{PE} = 1.0264$, which is smaller than the corresponding values of the other systems at $k = 8$.

6. Conclusions

The linking matrix can be used for the study of the entanglement in a system of closed, open or mixed chains, as in the cases of polymer chains in a melt or vortex filaments in a fluid flow. In the case of a system employing PBC, the periodic linking matrix can be used to reduce the study of the entanglement of the infinite periodic system to the study

of a finite dimensional matrix. The periodic linking matrix can be applied to open, closed, mixed or infinite chains in PBC. We discussed the dependence of the periodic linking matrix on cell size, and our numerical results on systems of random walks in PBC showed that there is a cell size after which the characteristic values of the periodic linking matrix converge to an asymptotic value. We suggested a method to extract information from the linking or the periodic linking matrix about the homogeneity of the entanglement in a physical system using graphs. Our numerical results showed that the asphericity of the eigenvalues of the periodic linking matrix, the Cheeger constant and the Laplacian matrix of the corresponding graphs can provide measures of the homogeneity of the entanglement of a collection of chains. Our numerical results also suggest that the homogeneity of the entanglement depends on chain length.

Acknowledgements

The authors are grateful to the Isaac Newton Institute for Mathematical Sciences and to the Organizers of the Programme "Topological Dynamics in the Physical and Biological Sciences" for hosting during the preparation of this paper. This research has been co-financed by the European Union (European Social Fund ESF) and Greek national funds through the Operational Program "Education and Lifelong Learning" of the National Strategic Reference Framework (NSRF) - Research Funding Program: Heracleitus II. Investing in knowledge society through the European Social Fund.

References

[1] de Gennes PG. *Scaling Concepts in Polymer Physics*. Cornell University Press Ithaca NY; 1979.
[2] Edwards F 1967 Statistical mechanics with topological constraints: I *Proc Phys Soc* **91** 513-9.
[3] Millett K., Dobay A. and Stasiak A. Linear random knots and their scaling behavior *Macromolecules* vol. 38. 2004. p. 601.
[4] Everaers R, Sukumaran SK, Grest GS, Svaneborg C, Sivasubranian A, Kremer K. Rheology and microscopic topology of entangled polymeric liquids *Science* vol. 303. 2004. p. 823.
[5] Kröger M. Shortest multiple disconnected path for the analysis of entanglements in two and three- dimensional polymeric systems *Comp. Phys. Commun.* vol. 168. 2005. p. 209.
[6] Tzoumanekas C and Theodorou DN. Topological analysis of linear polymer melts *Macromolecules* vol. 39. 2006. p. 4592.
[7] Panagiotou E., Millett KC. and Lambropoulou S. The linking number and the writhe of uniform random walks and polygons in confined spaces *J. Phys. A: Math. Theor.* vol. 43. 2010. p. 045208.
[8] Moffatt HK. The degree of knottedness of tangled vortex lines *J. Fluid Mech* vol. 35. 1969. p. 117-129.
[9] Moffatt HK and Ricca RL. Helicity and the Calugareanu Invariant *Proc. R. Soc. Lond. A* vol. 439. 1992. p. 411-429.
[10] Bajer K. Abundant singularities. *Fluid Dynamics Research* vol. 36(4-6). 2005. p. 301-327.
[11] Sreenivasan KR and White CM. The onset of drag reduction by dilute polymer additives, and the maximum drag reduction asymptote *J Fluid Mech*vol. 409. 2000. p. 149-164.
[12] Orlandini E and Whittington SG. Entangled polymers in condensed phases *J. Chem. Phys.* vol. 121. 2004. p. 12094-99.
[13] Berger MS. Magnetic helicity in a periodic domain *J. Geoph. Res.* vol. 102:A2. 1997. p. 2637-3644.
[14] Morton HR and Grishanov S. Doubly Periodic Textile Structures *J. Knot. Theory Ramif.* vol. 18: 12. 2009. p. 1597-1622.
[15] Qin J and Milner ST. Counting polymer knots to find the entanglement length *Soft Matter* vol. 7. 2011. p. 10676-93.
[16] Panagiotou E, Tzoumanekas C, Lambropoulou S, Millett KC and Theodorou DN. A study of the entanglement in systems with periodic boundary conditions *Prog. Theor. Phys. Supplement* vol. 191. 2011. p. 172-181.
[17] Panagiotou E. *Topological Methods for Measuring the Entanglement in Polymers*, PhD Thesis, National Technical University of Athens 2012.
[18] Berger MA and Field GB. The topological properties of magnetic helicity *J Fluid Mech* vol. 147. 1984. p. 133-148.
[19] Hunt JCR and Hussain FA. Note on velocity, vorticity and helicity of inviscid fluid elements *J Fluid Mech* vol. 229. 1991. p. 569-587.
[20] Arnold VI. The Asymptotic Hopf invariant and its applications *Sel. Math. Sov.* vol. 5;4 1986.
[21] Moffatt HK. The energy spectrum of knots and links *Nature* vol. 347 . 1990. p. 367-369.
[22] Moffatt HK. Magnetostatic equilibria and analogous Euler flows with arbitrary complex topology. Part I. Fundamentals. *J. Fluid. Mech.* vol. 159 . 1985. p. 359-378, Moffatt HK. Magnetostatic equilibria and analogous Euler flows with arbitrary complex topology. Part II. Stability Considerations. *J. Fluid. Mech.* vol. 166 . 1986. p. 359-378.
[23] Calugreanu G 1961 Sur les classes d'isotopie des noeuds tridimensionnels et leurs invariants *Czechoslovak Mathematical Journal* **11** 588-625
[24] Banchoff T 1976 Self linking numbers of space polygons *Indiana Univ. Math. J.* **25** No. 12 1171-88.
[25] Bastide J, Boué F, Mendes E, Zielinski F, Buzier M, Lartigue C et al. Is the distribution of entanglements homogeneous in polymer melts? *Progr. Coll. Pol. Sc.* vol. 91. 1993. p. 105-108.
[26] Brouwer AE and Haemers WH. *Spectra of Graphs* Springer XIII; 2012.
[27] Theodorou DN and Suter UW. Shape of unperturbed Linear Polymers: Polypropylene *Macromolecules* vol. 18. 1985. p. 1206-14.
[28] Rawdon EJ, Kern JC, Piatek M, Plunkett P, Stasiak A and Millett KC. Effect of knotting on the shape of polymers *Macromolecules* vol. 41. 2008. p. 8281-87.

Subject index

Author index